(1)

LA-8827-MS

Geologic and Geophysical Investigations of the Zuni-Bandera Volcanic Field, New Mexico

LA--8827-MS

DE81 023984

University of California

LOS ALAMOS SCIENTIFIC LABORATORY

Post Office Box 1663 Los Alamos, New Mexico 87545

DISCLAIMER

Edited by

Glenda Cremer
Group G-1

This work was supported by the US Department of Energy, Division of Geothermal Energy.

UNITED STATES
DEPARTMENT OF ENERGY
CONTRACT W-7405-ENG. 36

LA-8827-MS

UC-66b
Issued: May 1981

Geologic and Geophysical Investigations of the Zuni-Bandera Volcanic Field, New Mexico

Mark E. Ander
Grant Heiken
John Eichelberger*
A. W. Laughlin
Stephen Huestis**

*Sandia National Laboratories, Albuquerque, NM 87185
**Geology Department, University of New Mexico, NM 87131.

GEOLOGIC AND GEOPHYSICAL INVESTIGATIONS OF THE ZUNI-BANDERA VOLCANIC FIELD, NEW MEXICO

by

Mark E. Ander, Grant Heiken, John Eichelberger,
A. W. Laughlin, and Stephen Huestis

ABSTRACT

A positive, northeast-trending gravity anomaly, 90 km long and 30 km wide, extends southwest from the Zuni uplift, New Mexico. The Zuni-Bandera volcanic field, an alignment of 74 basaltic vents, is parallel to the eastern edge of the anomaly. Lavas display a bimodal distribution of tholeiitic and alkalic compositions, and were erupted over a period from 4 Myr to present. A residual gravity profile taken perpendicular to the major axis of the anomaly was analyzed using linear programming and ideal body theory to obtain bounds on the density contrast, depth, and minimum thickness of the gravity body. Two-dimensionality was assumed. The limiting case where the anomalous body reaches the surface gives 0.1 g/cm³ as the greatest lower bound on the maximum density contrast. If 0.4 g/cm³ is taken as the geologically reasonable upper limit on the maximum density contrast, the least upper bound on the depth of burial is 3.5 km and minimum thickness is 2 km. A shallow mafic intrusion, emplaced sometime before Laramide deformation, is proposed to account for the positive gravity anomaly. Analysis of a magnetotelluric survey suggests that the intrusion is not due to recent basaltic magma associated with the Zuni-Bandera volcanic field. This large basement structure has controlled the development of the volcanic field; vent orientations have changed somewhat through time, but the trend of the volcanic chain followed the edge of the basement structure. It has also exhibited some control on deformation of the sedimentary section.

I. INTRODUCTION

The Zuni-Bandera volcanic field consists of a northeast-trending chain of late Cenozoic basaltic vents and related lava flows, forming a band 90 km long and 1 to 15 km wide. It is located along the southeastern edge of the Colorado Plateau and forms part of the Jemez volcanic lineament,[1-3] which strikes approximately N52°E (Fig. 1.). The elongate Zuni-Bandera volcanic field is not parallel to the Jemez lineament but is oblique to it. It is, however, parallel to a major basement structure associated with a large positive gravity anomaly. The volcanic field is also parallel to northeast-trending normal faults that cut some of the older volcanic rocks of the field. The field overlies a section of Permian through Mesozoic age sedimentary rock units, which are exposed along the flanks of the Zuni uplift. The northernmost vents in the field are located along N-S striking faults that cut the Precambrian igneous and metamorphic complex exposed in the core of the uplift.[4]

The Zuni Mountains area is marked by relatively high heat flow.[5] Edwards et al.[5] found that heat flow values of 83.6 to 125.4 mW/m^2 are characteristic

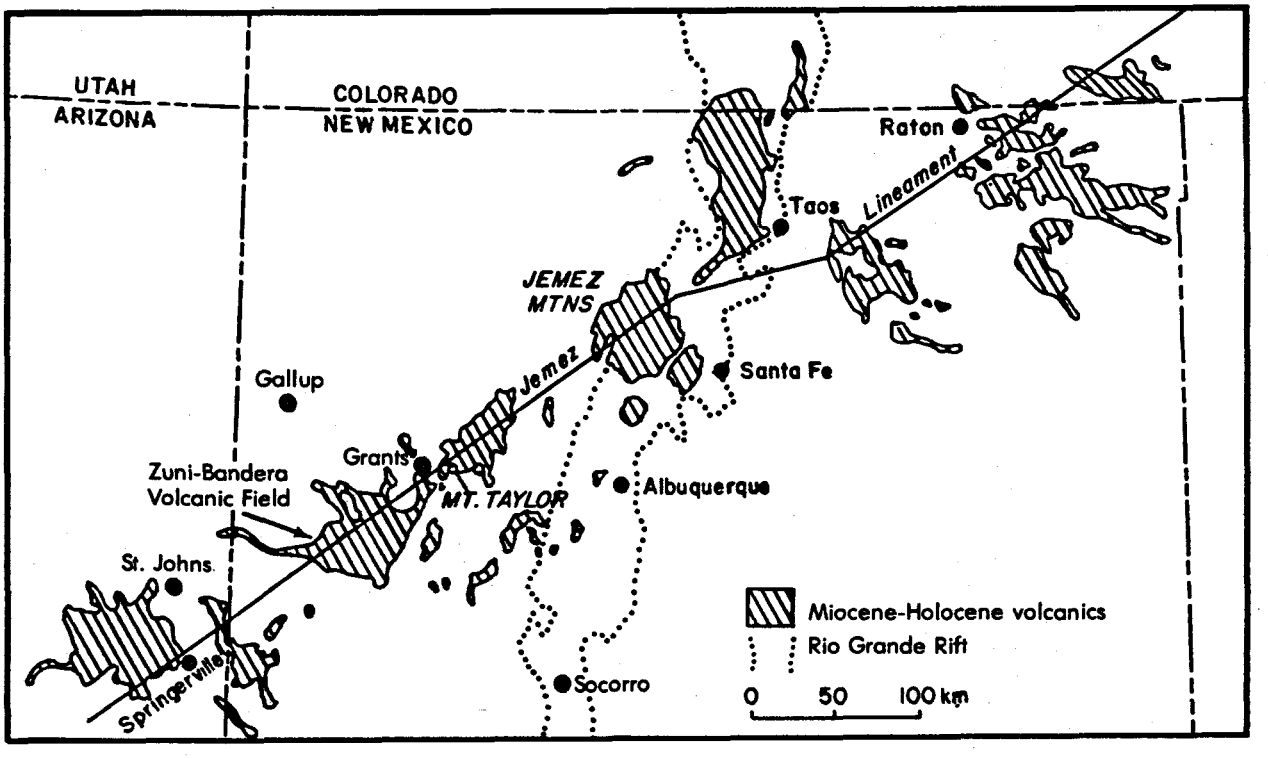

Fig. 1.
The Jemez lineament showing the Miocene-to-Holocene volcanic rocks. (Modified from Chapin et al.[13]).

of the flanks of the uplift. Levitte et al.[6] performed a thermal gradient survey of the wells in the general area around the Zuni Pueblo and found gradients substantially above normal (>25°C/km). Unfortunately, very few of these wells are within the volcanic field itself.

This study examines the structure, petrology, and age of the basaltic flows and their vents in an effort to determine the duration and style of volcanism. Gravity analysis was used to delineate basement structures that apparently localized the volcanism. Magnetotellurics (MT) was used to search for electrical conductive anomalies that may be correlated with gravity anomalies. These MT data come from part of a regional deep MT survey, conducted by Los Alamos National Laboratory in west-central New Mexico. The regional MT survey is being used to define the depth of a crustal deep-electrical conductor beneath the region and to attempt a correlation of this conductor with other geological and geophysical data sets, the heat flow in particular.[7-9] This study is part of a larger regional MT study of Arizona and New Mexico.[9-12]

II. DESCRIPTION OF THE VOLCANIC FIELD

Parts of the Zuni-Bandera volcanic field cross four 1° x 2° quadrangles; there are geologic compilations for three of them--Gallup, Socorro, and Albuquerque.[14-16] A geologic compilation for the St. Johns quadrangle is incomplete. Parts of the volcanic field have been described by Laughlin and coworkers.[2,17-21] Characteristics of the lava flows, so beautifully displayed at Bandera Crater and along Interstate Highway 40 near Grants, have been described by Nichols[22] and Hathaway and Herring.[23]

The chain of vents is oriented N38°E, with the exception of a north-south segment that crosses the Zuni uplift (Fig. 2). This north-south vent segment across the uplift follows some visible faults.[4] The more numerous northeast-trending normal faults and vents are parallel to a prominent gravity anomaly, the Chimney Hill gravity high.[9,24] This anomaly is 90 km long and 30 km wide and extends southwest from the southern edge of the Zuni uplift. The volcanic chain follows the eastern edge of the anomaly.

There are 74 vents in the field; all have erupted lavas and tephra of basaltic composition. Vent types include simple cinder cones, spatter ramparts and cones, small shields, maars, and collapse pits. Descriptions of the vents are summarized in Appendix A.

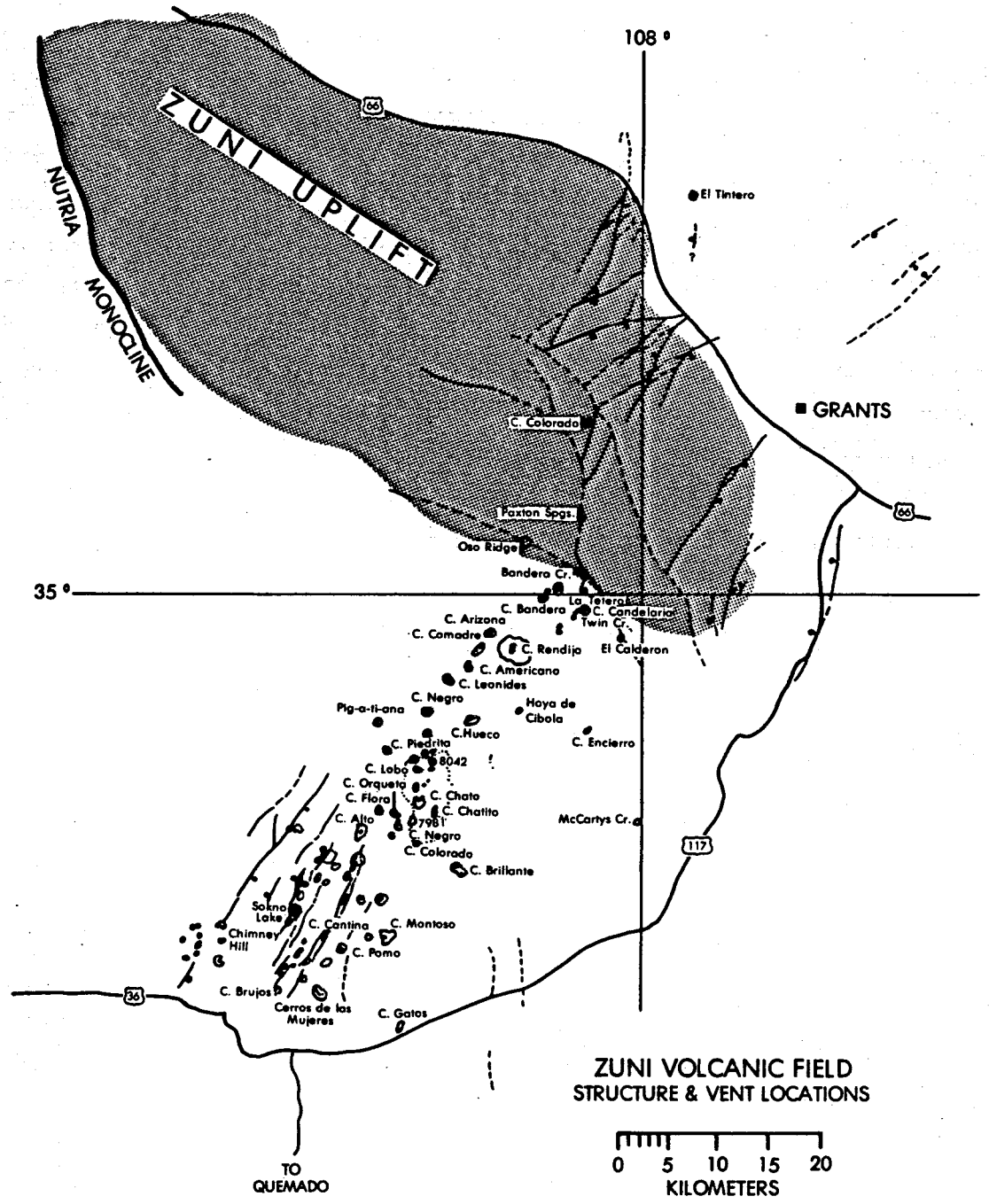

Fig. 2.
Map of Zuni volcanic field structure and vent locations. Faults are marked with solid lines and dashed lines where inferred. Cones are marked with solid lines. Maars are marked with solid lines and depression symbols.

Lava flows were not mapped. Only the youngest flows, those associated with the McCartys vent and the cluster of cones near Bandera Crater, are easily mapped. Most others are difficult to trace to their sources because they are either buried by younger flows or masked by soil and sediments. Lava flows follow drainages east and west from the axis of the chain, which also coincides with, and marks, the Continental Divide. The McCartys flow and the underlying Laguna flow fill much of the valley east of the chain. The McCartys flow continues down the Rio San Jose Valley toward McCartys, an overall distance of 50 km. The Fence Lake flow drained west, past the Arizona border, a distance of 90 km. Another group of unnamed lava flows is located between Bandera Crater and Zuni Pueblo. These flows could have originated from any of the several dozen vents in the middle of the volcanic field.

The approximate total area covered by lavas from the Zuni-Bandera field, including flows from El Tintero, is 2460 km^2. There are very few composite thickness measurements available; 61 m at El Morro, New Mexico; 20 to 60 m near Grants, New Mexico; and 36 m near the center of the El Tintero flow near Blue Lake, New Mexico. If the average thickness of erupted lavas for the field is assumed to be 50 m, the total volume of lavas is 123 km^3; if the average thickness is one-half of that, it is about 62 km^3. With 74 vents, the lower approximation may be closer to reality, with an average volume of lava and pyroclastics per vent of about 0.85 km^3. For comparison, the total volume of lava and pyroclastics erupted at Paricutin, Mexico, was 1.8 km^3.[25]

Vent elongations were measured wherever possible (Table I). Because our observations showed most basaltic magma moved up along fissures, the elongation measurements provide some data on the nature of the fault and joint systems under the field. Only a small number of cones are symmetrical. Vent elongations range from N-S to N45°E, with most parallel to the long axis of the volcanic chain (N38°E) and to normal faults exposed in the southern part of the field. Three major exceptions are Cerro Brillante and Cerro Pomo, both with vent elongations of N38°W, and Cerros de la Mujeres with vent elongation of N45°W.

III. AGE OF THE ACTIVITY

Because all of the vents are in the same climatic zone and composed of similar basalt types, we are able to assign relative ages to nearly all of them (Table I). These ages range from young cones that exhibit little erosion

TABLE I

ZUNI-BANDERA VOLCANIC FIELD - VENT CHARACTERISTICS

Vent	Little Vegetation, Very Little Erosion	Little Erosion, Well-Developed Soil and Vegetation	Eroded Crater Preserved	Eroded, Crater Eroded Away Not Faulted	Eroded, Crater Eroded Away Faulted	Eroded, Vent Exposed (Mesa)	Vent Elongations
El Tintero		x (0.4 Myr)					N8°w
Cone near Cerro, Colorado			x				N3°W
Paxton Springs		x					N11°E
Oso Ridge			x				N-S
Bandera Crater	x (1000 yr)						N32°E
Cerro Bandera		x					N5°E
Lava Crater (La Tetara)	x						Symm.
Cone E of Lava Crater (Cerro Candelaria)	x						N26°E
Twin Craters		x					N25°E
Crater S. of Twin Craters		x					N35°E
Crater SE of Twin Craters (El Calderon)		x					N25°E
Hoya de Cibola	x						N37°E
Cerro Rendija			x				N-S
Cerrito Arizona			x				N30°E
Cerrito Comadre				x			N33°E
Cerro Americano			x				Symm.
Cerro Leonides				x			N25°E
Cerro Piedrita			x				N30°E
Cone 2-1/2 km NW of C. Piedrita			x				N40°E
Cerro Lobo			x				N22°E
Hill 8042				x			N45°E
Pig-a-ti-ana			x				N30°E
Cerro Negro			x				N14°E
Cerro Hueco			x				N5°E
Cerro Chato			x				N-S
Cerro Chatito					x		?
Cerro Brillante			x (0.94 ±0.4 Myr)				N38°W
Cerro Colorado				x			N-S
Cerro Negro			x				N12°E
Hill 7981 (E of C. Negro)					x		N14°E
Cerro Flora			x				N25°E
Cerro Orqueta			x				N30°E
Cerro Alto		x(1.5±0.3 Myr)	x				N32°E
Maar S. of C. Alto			X (?)				N25°E

TABLE I (cont)

ZUNI-BANDERA VOLCANIC FIELD - VENT CHARACTERISTICS

Vent	Little Vegetation, Very Little Erosion	Little Erosion, Well-Developed Soil and Vegetation	Eroded Crater Preserved	Eroded, Crater Eroded Away Not Faulted	Eroded, Crater Eroded Away Faulted	Eroded, Vent Exposed (Mesa)	Vent Elongations
Spatter Ramparts S. of C. Alto				x			N25°E
Crater 2 km SW of C. Alto				x			N34°E
Two Vents, S. of Laguan Colorado				x			Symm.
Two Vents SW of C. Alto Maar				x			N45°E
Vent West of C. Alto Maar					x		N40°E
Two Spatter Ridges N. of Sokno Lake					x		Symm.
					x		N30°E
Chimney Hill				x			N35°E
Sokno Lake Maar + Cinder Cone					x		N31°E
Cerro Cantina					x		N31°E
Two Cones W of C. Cantina					x		N30°E
Cerro Brujos				x			?
Cerro Montoso			x				Symm.?
Cerro Pomo			x				Symm.?
Cerros de la Mujeres						x (16.7±0.8 Myr)	N38°W
						x (15.5±0.8 Myr) (17.0±0.8 Myr)	N45°W
Cone SW of Cerro Pomo .				x			Symm.
Cerro Gatos				x			N-S?

and little or no soil to those where only resistant plugs remain. The only example of the latter is a pair of older vents at Cerros de la Mujeres, dated at 27 Myr that are not part of the main volcanic field.

Geomorphically, the volcanic chain generally is younger from south to north (Table I). With the exception of Cerro Pomo and the Chimney Hill cluster, most of the vents in the southern part of the field are deeply eroded and cut by normal faults. In the central part of the field, the vents are eroded and have a well-developed soil profile, but are not cut by normal faults. Two of these vents have been dated: Cerro Brillante, 0.94 ± 0.4 Myr and Cerro Alto, 1.5 ± 0.3 Myr. Laughlin et al.[26,27] dated vents in the central part of the chain at 3.8 ± 0.40 Myr, 1.41 ± 0.29 Myr, 1.57 ± 0.26 Myr, and 0.70 ± 0.55 Myr. The northern part of the chain is younger, with well-preserved cinder cones and spatter ramparts. These range in age from 0.199 ± 0.042 Myr for an alkalic flow beneath Bandera Crater, New Mexico,[28] to 700 A.D., an archaeological date for the McCartys flow.[22] An alkalic flow, near Laguna Pueblo northeast of the Zuni-Bandera field, has an age of 0.38 ± 0.25 Myr.[27] The source for this flow is probably not within the field.

The Zuni-Bandera volcanic field was active from around 4 Myr to about 1000 years ago. This activity was contemporaneous with volcanic activity elsewhere along the Jemez volcanic lineament; the Mt. Taylor field, located immediately northeast of the chain was active from 3.5 to 1 Myr and the Springerville field, located southwest, erupted from about 3 Myr to 22,000 yr b.p.[3,26]

IV. PETROLOGY OF THE LAVAS

Field observation shows nearly all of the lavas to be aphanitic, with only a trace of visible olivine phenocrysts and a few quartz xenocrysts. For field descriptions, see Appendix A. Table II is a petrologic summary. Most of the basalts can be characterized as having greater than 85% finely crystalline groundmass, with small phenocrysts of olivine, pyroxene, and plagioclase. An exception to this general characterization is the stubby lava flow from the Cerro Chato-Cerro Lobo cluster, where the lavas have abundant large plagioclase phenocrysts.

Xenoliths and xenocrysts are rare and consist of mostly quartz and granitic or granodioritic fragments, probably from the basement complex. Xenoliths from Cerro Piedrita consist of partly melted granodiorite. Laughlin et

TABLE II

ZUNI-BANDERA VOLCANIC FIELD - PETROLOGIC SUMMARY

	Mode						Description								
	Phenocrysts						Phenocryst Size (mm)			Phenocryst Shape					
Location	Ol	Pyx	Pl	Op	Xeno-crysts	Matrix	Ol	Pyx	Pl	Ol	Pyx	Pl	Matrix	Xenoliths	Comments
Zuni Canyon flow (Paxton Spgs)	10	-	0.1	-	-	89.9	0.4/1.3	-	0.1	eu., w/res.	-	eu	x	-	picotite in Ol.
Paxton Springs	11	tr	tr	-	-	88.3	0.3/1.8	0.1	0.1	eu., w/res.	eu	eu	fx	Qtz-Feld	picotite in Ol.
C Colorado (north)	12	tr	0.1	-	-	87.9	0.1/2.0	0.4	0.4	eu	eu	eu lath	fx	-	-
El Tintero	2.7	0.8	13.1	-	-	83.4	0.8/2.0	1.5/2.0	4.0/6.0	eu-skel.	sub-ragged	lath	gl	-	-
C. Oso flow	7.3	-	-	-	-	92.7	0.1/0.6	-	-	eu	-	-	fx	-	some Pl. in cone cinders
C. Rendija	3.9	3.8	-	-	-	92.7	1.0/2.0	2.0	-	eu	rounded	-	fx	-	Pyx in single clot. Oxidized Ol.
Bandera Crater	10.5	-	-	-	-	89.5	0.2/1.0	-	-	eu-skel.	-	-	fx	-	-
Twin Craters	10.9	-	-	-	-	89.1	0.5/1.5	-	-	eu	-	-	fx	-	-
C. Alto	6.0	1.0	0.4		Qtz-0.6 San-0.2 Pl.-0.2	91.6	0.4/1.0	0.1	0.1	sub.	ragged	eu + resorb.	fx	-	Qtz + San. with Pyx rims
NNE of C. Chato	3.8	2.6	21.8	-	Pl.-0.4	71.4	0.5/1.0	1.0/2.0	1.0/2.0	sub.	ragged	long eu. laths	fx	-	Pl. + Ol. + Pyx. clots. Some Cpx rims on Ol. Some Cpx clots
Ridge E. of C. Negro	4.6	0.6	15.8	0.2	-	78.8	0.5	0.5	0.5/3.0	sub (some resorp.)	ragged	long eu.	fx/gl	-	Pl. + Ol. + Pyx. clots. Some Cpx rims on Ol. Some Cpx clots
Sokno Lake	9.8	-	-	-	Qtz-tr.	90.2	0.2/3.0	-	-	some eu. some skel.	poik.	-	fx	-	
C. Chatito	9.6	-	-	-	Qtz-0.6 Pl.-0.4	89.4	0.2	-	-	eu-skel.	-	-	fx	Qtz-Feld	Qtz/Feld basement xenos.
N. of C. Chato	12.4	-	4.4	-	-	83.2	0.2/1.0	-	0.5/1.0	sub-	-	long laths	fx	-	-
NNE of C. Chato	2.5	3.7	11.3	-	-	82.5	0.2/1.0	0.2	0.5/1.5	sub	ragged	very long laths	gl	Cpx	Pl. + Ol. clots Cpx from xenol.?
C. Lobo	4.0	2.0	16.0	-	-	78.0	0.5	1.0/2.0	1.0/3.0	sub-embayed	large, round	long laths	fx	-	Some Pl. + Ol. clots
C. Hueco	14.0	-	6.0	-	-	80.0	0.4/1.0	-	0.5-1.0	sub-embayed	-	long laths	cx	-	-
NE of C.Piedrita	5.0	-	2.2	-	resorb. Pl.-1.8 res. Pl. -0.2	91.0	0.5/1.0	-	0.5	sub-embayed	-	long laths	fx	-	Pl. + Ol. clots Pl. not well-developed
C. Piedrita	7.0	1.0	-	-	Qtz-0.2	91.6	0.2/1.0	0.15	-	sub-embayed	sub-eu.	-	fx	melted Qtz -Feld.	Small, melted base-ment frags.
C. Pomo	6.6	1.2	-	-	Qtz-2.0	90.2	0.2/1.0	-	-	eu, sub, skel.	rims on Qtz	-	fx	Dunite	Qtz prob. not magmatic

TABLE II (cont)

ZUNI-BANDERA VOLCANIC FIELD - PETROLOGIC SUMMARY

	Mode						Description								
	Phenocrysts						Phenocryst Size (mm)			Phenocryst Shape					
Location	Ol	Pyx	Pl	Op	Xeno-crysts	Matrix	Ol	Pyx	Pl	Ol	Pyx	Pl	Matrix	Xenoliths	Comments
C. Mujeres (old)	7.8	9.0	-	-	-	83.2	0.4/1.0	0.4/3.0	-	sub.	eu, some resorb	-	fx	Cpx?	Qtz-Feld, vesicle filling
C. Flora	6.8	-	-	-	-	93.2	0.2/1.0	-	-	eu, sub skel.	-	-	fx	-	-
C. Orqueta	2.6	3.6	0.2	-	Pl.-tr. Qtz-0.6	93.0	0.5/1.0	0.2+rims	0.5	sub, embayed	sub,eu + rims	laths (thin)	fx	Qtz-Pyx	Coarser matrix around Ol.
S. of C. Alto Maar	2.2	0.2	-	-	-	97.6	0.2/0.5	0.1	-	skel.	-	-	fx	-	Ol. clots
C. Brillante	11.2	-	-	-	Qtz-0.8	88.0	0.8/0.2	-	-	sub	-	-	fx	-	rdd. Qtz xeno. Probably not magmatic
C. Americano	8.8	-	0.2	-	Qtz-tr.	91.0	0.2/1.0	-	0.5	sub-skel.	-	lath	fx	-	Qtz-basement fragment
C. Negro-North	15.8	-	0.2	-	-	84.0	0.3/5.0	-	1.0	sub.	-	lath	cx	-	-
C. Negro-Central	6.0	-	-	-	Qtz-0.6	93.4	0.3/0.8	-	-	sub-eu	-	-	fx	-	Qtz with Pyx rims
C. Colorado-South	9.0	-	0.2	-	Qtz-0.2	90.6	0.2/1.0	-	-	sub-eu some embayed	-	-	fx	-	Large embayed Ol.
S.C. Brillante	7.8	-	-	-	-	92.2	0.2/1.0	-	-	sub	-	-	fx	-	Altered
C. Gatos	2.4	-	8.8	-	-	88.8	0.4/2.0	-	1.0/2.0	sub-eu	-	long laths	cx	-	Ol. + Pl. glomerocrysts
C. Leonides	3.2	1.0	-	-	-	95.8	0.1/1.0	2.0	-	sub	anhed.	-	fx+ gl	1 Pyx xeno	Variable matrix
NNE of C. Piedrita	7.2	-	3.0	-	-	89.8	0.3/1.0	-	0.4/0.7	anh.-embayed	-	laths	fx	-	Pl. + Ol. clots
E. of C. Piedrita	11.0	0.2	0.2	-	-	88.6	0.2/1.0	0.2	0.1	eu	eu	equant	fx	-	Highly oxidized Ol.
C. Comadre	6.4	-	0.4	-	-	93.2	0.3/1.0	-	0.5	sub-skel. embayed	-	laths	gl	-	Scoria

Explanation:

Mode - Ol = olivine, Pyx = pyroxene, Pl = plagioclase, Op = opaque oxides, Qtz = quartz, San. = sanidine, Cpx = clinopyroxene, tr. = trace. Phenocrysts are defined as grains 0.1 mm.

Shape - sub = subhedral, eu = euhedral, anh = anhedral, skel = skeletal, res = resorbed, poik = poikilitic.

Matrix - fx = fine-grained, crystalline; cx = coarse-grained, crystalline; gl = glass.

al.[2,29] have described ultramafic xenoliths in bombs from Bandera Crater. We found only one small dunite xenolith in lavas from Cerro Pomo.

Samples were sent to two laboratories for major element analysis (J. Husler, University of New Mexico and P. Hooper, Washington State University). The new analyses, plus a compilation of existing chemical data for the Zuni-Bandera field, are presented in Table III.

The basaltic lavas show a bimodal distribution of alkalic to tholeiitic basalts. Norms calculated by D. Vaniman[30] and other workers[2,17,19,20] indicate a range of compositions from nepheline to hypersthene to quartz normative. There is no systematic variation of basalt compositions with time, vent type, or position within the field. Variation appears to be random.

V. GRAVITY ANALYSIS

The source vents for the Zuni volcanic field are superimposed on the Bouguer anomaly gravity map in Fig. 3. The gravity data used in the production of the map come from the Defense Mapping Agency gravity data bank.

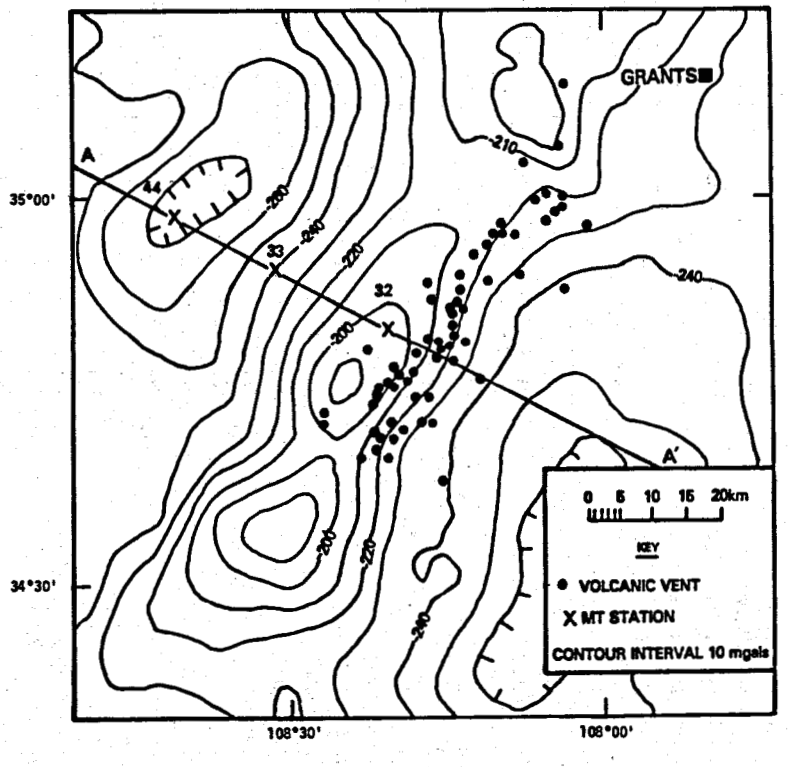

Fig. 3.
Bouguer gravity anomaly map of Chimney Hill gravity high showing Zuni volcanic vent locations. Gravity profile AA' is shown in Fig. 4 (from Ander[9]).

TABLE III

COMPOSITION OF LAVAS FROM THE ZUNI-BANDERA VOLCANIC FIELD

Name of Vent	SiO_2	Al_2O_3	Fe_2O_3	FeO	MgO	CaO	Na_2O	K_2O	TiO_2	MnO	P_2O_5	Total	Type of Sample	Reference	No. Samples
El Tintero	49.9	15.6	2.9	8.4	8.4	8.9	3.1	0.78	1.5	0.17	0.32	99.97	lava	21	1
C. Colorado (N) (mean)	45.4	14.5	- 10.4 -		10.3	9.6	3.28	1.62	2.19	0.18	-	97.47	lavas	17	25
C. Colorado (N) (std. dev.)	0.8	0.26	- 0.12-		0.4	0.23	0.37	0.2	0.16	0.00	-	-	-	-	-
Paxton Springs (S) (mean)	45.6	15.6	- 10.8 -		9.13	9.29	3.46	1.62	2.75	0.23	-	98.48	lavas	17	10
Paxton Springs (S) (std. dev.)	0.41	0.25	- 0.33-		0.35	0.33	0.37	0.1	0.1	0.01	-	-	-	-	-
Paxton Springs (N) (mean)	45.3	15.6	- 10.6 -		9.76	9.61	2.95	1.46	2.65	0.24	-	98.17	lavas	17	14
Paxton Springs (N) (std. dev.)	0.82	0.58	- 0.56-		0.46	0.22	0.42	0.16	0.24	0.01	-	-	-	-	-
C. Bandera	49.5	15.6	- 9.78-		9.72	8.42	3.01	1.31	2.02	0.15	-	99.51	lava	31	1
C. Bandera	49.4	15.9	9.91	-	9.79	8.67	3.37	1.50	2.07	6.16	-	100.77	lava	31	1
Bandera Crater	44.85	15.10	3.16	8.90	10.76	9.47	3.46	1.36	2.39	0.17	0.37	99.62	cinders	2	1
Bandera Crater	44.47	15.22	4.39	8.42	9.30	8.80	3.38	1.60	3.04	0.15	0.58	99.35	lava	2	1
McCarty's Crater	49.93	16.62	1.54	9.25	8.45	8.90	2.89	0.75	1.38	0.17	0.25	100.13	lava	20	1
La Tetera	48.5	15.30	- 11.4 -		9.57	9.11	2.94	0.69	1.44	0.16	-	99.11	lava	2	1
El Calderon	50.18	15.15	- 11.3 -		8.44	8.92	3.14	0.72	1.57	0.15	-	99.57	lava	2	1
Hoya de Cibola	50.57	15.44	- 10.4 -		8.12	9.45	2.75	0.44	1.26	0.14	-	98.57	lava	2	1
Cerrito Arizona	50.2	15.4	- 10.6 -		9.23	9.09	2.91	0.86	1.45	0.15	-	99.89	lavas	31	10
Cerrito Comadre	49.2	15.0	- 10.4 -		9.39	9.09	2.67	0.82	1.62	0.16	-	98.35	lavas	31	2
Cerro Americano	49.0	15.0	- 10.2 -		10.4	8.7	2.3	1.05	2.0	0.16	-	98.81	lavas	31	2
Cerro Leonides	47.7	14.7	- 10.9 -		12.5	9.4	2.61	1.34	2.14	0.17	-	101.46	lavas	31	4
C. Piedrita	47.83	14.97	- 11.3 -		8.83	8.95	3.86	1.44	2.16	0.17	0.52	100.06	lava	a	1
C. Lobo	52.82	15.96	- 10.9 -		5.86	9.08	3.45	0.72	1.44	0.17	0.30	100.71	lava	a	1
C. Lobo	51.31	16.01	5.19	5.50	6.60	9.20	2.70	0.71	1.28	0.14	0.25	99.54	lava	b	1
C. Negro (N)	46.2	15.4	- 10.8 -		10.0	8.71	2.59	1.43	2.56	0.16	-	97.85	lava	31	4
C. Hueco	48.1	15.9	- 11.4 -		10.7	9.35	2.69	0.82	1.57	0.17	-	100.7	lava	31	3
C. Hueco	49.65	15.41	- 11.7 -		8.43	8.69	3.36	0.91	1.63	0.17	0.42	100.35	lava	a	1
Cone 2-1/2 km N. C. Piedrita	49.0	15.0	- 10.6 -		10.4	9.1	3.04	1.61	2.31	0.16	-	101.22	lavas	31	2
C. Chato	47.9	15.42	- 12.0 -		6.71	7.86	4.53	2.16	2.20	0.19	0.62	99.58	lava	a	1
C. Chato	46.89	15.30	10.92	1.19	7.55	7.77	4.03	2.02	2.13	0.18	0.63	99.54	lava	b	1
C. Lobo Shield	53.11	16.79	- 11.07-		5.44	8.61	3.69	1.06	1.70	0.16	0.33	101.96	lava	a	1
C. Brillante	49.47	14.74	- 10.5 -		8.33	8.34	3.86	1.82	2.17	0.16	0.54	99.93	lava	a	1
C. Brillante	47.89	14.52	4.79	6.69	9.49	8.34	3.31	1.76	2.12	0.16	0.59	99.65	lava	b	1

TABLE III (cont)

COMPOSITION OF LAVAS FROM THE ZUNI-BANDERA VOLCANIC FIELD

Name of Vent	SiO_2	Al_2O_3	Fe_2O_3	FeO	MgO	CaO	Na_2O	K_2O	TiO_2	MnO	P_2O_5	Total	Type of Sample	Reference	No. Samples
C. Colorado (S)	46.83	15.82	11.5		8.63	8.8	3.89	1.61	2.35	0.18	0.57	99.27	lava	a	1
C. Negro	47.55	15.2	11.1		9.32	8.98	3.62	1.39	2.13	0.17	0.5	99.91	lava	a	1
C. Orqueta	51.78	15.43	10.6		6.94	7.75	4.28	1.87	1.79	0.16	0.44	100.99	lava	a	1
C. Alto	55.75	15.58	8.9		5.71	7.45	4.16	1.84	1.67	0.14	0.36	101.51	lava	a	1
C. Alto	54.07	15.10	1.69	6.82	6.32	7.34	3.61	1.76	1.56	0.13	0.38	99.67	lava	b	1
C. Montoso	51.78	16.49	10.4		5.92	9.92	3.49	0.72	1.73	0.17	0.32	100.97	lava	a	1
C. Pomo	55.10	14.98	8.9		6.33	7.28	3.86	1.79	1.58	0.13	0.33	100.25	lava	a	1
Cerros Gatos	53.49	15.8	10.7		5.33	9.44	3.61	0.75	1.59	0.16	0.23	101.06	lava	a	1
C. de la Mujeres	50.89	10.56	8.4		9.31	8.94	3.30	4.57	2.30	0.13	1.05	99.42	lava	a	1

[a]Source is this paper, analysis performed by P. R. Hooper, Washington State University.

[b]Source is this paper, analysis performed by J. Husler, University of New Mexico.

Also shown on the map are the locations of the deep magnetotelluric sites discussed in this paper. A positive northeast-trending gravity anomaly, the Chimney Hill gravity high, extends southwest from the Zuni uplift. The anomaly is 90 km long and 30 km wide. The Zuni volcanic vents are parallel to the eastern edge of this anomaly, suggesting a causal relationship between the location of the vents and the orientation of the structure producing the gravity anomaly.

A gravity profile A-A' perpendicular to the major axis of the anomaly was selected for analysis. One of the most important problems in the interpretation of gravity measurements is that of separating the surface gravity field into its independent components and ascribing geological structures to each of the parts. For this study the regional component was obtained from the Bouguer gravity by a simple smoothing technique. Figure 4 shows the gravity profile A-A' and the assumed regional gravity anomaly. The regional gravity anomaly was chosen in such a way as to best reflect the long wavelength structure of the gravity signal, which at the same time produces a reasonably conservative estimate of the residual.

Conventional analysis of gravity data typically involves the construction of a density solution or suite of solutions that satisfy the data. It is well known, however, that even perfect (complete and accurate) gravity data are compatible with an infinite number of solutions. In practice, data necessarily comprise only a finite number of uncertain measurements so the nonuniqueness is even greater. A more acceptable analytical approach is therefore the recovery of properties shared by all solutions, or by some subset of solutions satisfying a priori restrictions. The properties to be treated here are greatest lower bounds on the maximum density of solutions confined to some prescribed region; if such a bound can be found, any solution confined to that region somewhere has a density reaching or exceeding the bound. For a given data set and region of confinement, the unique extremal solution with the smallest possible maximum density is termed the "ideal body" for that region. The theory of ideal bodies is developed by Parker.[32,33] Safon et al.[34] discuss the use of linear programming[35] for discovering the value of the bound.

The seven residual data points of Fig. 4 have been analyzed using ideal body theory to determine bounds on the density contrast, and using these bounds to derive maximum depth of burial and minimum thickness of the source. In all calculations, two dimensionality has been assumed, with densities

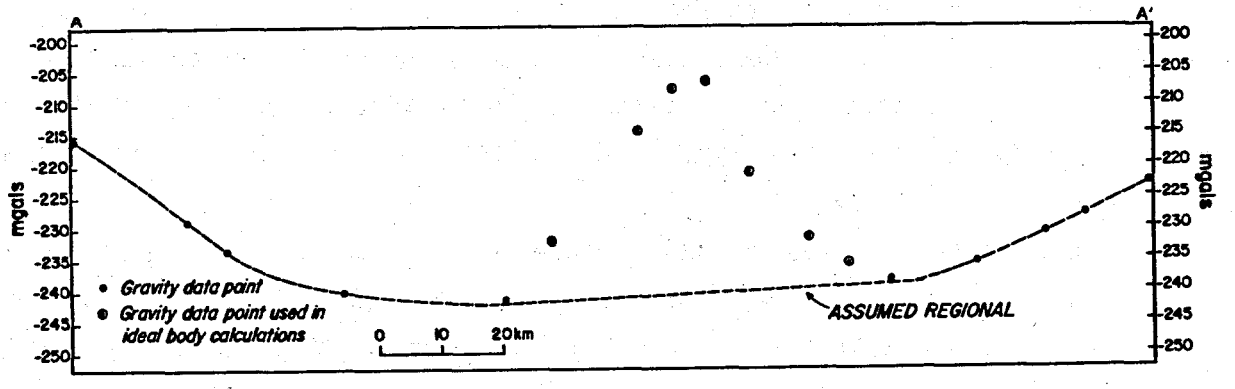

Fig. 4.
Chimney Hill gravity anomaly profile AA' showing assumed regional anomaly (from Ander[3]).

uniform in the horizontal direction perpendicular to the profile. Had more data been used, the derived bounds would necessarily have been more stringent. However, experience shows that measurements in excess of about five values do little to change the bounds unless the additional data deviate substantially from the trend already established. The two measurements on the flanks of the residual anomaly were not treated, due to their large relative uncertainties caused by uncertainty in the choice of a regional gravity anomaly. Details of the partitions used in the calculations are given in Appendix B.

Figure 5 plots density bounds as a function of depth to the top of the region of confinement of solutions. The curve must increase monotonically because each such region is a subset of all regions with shallower tops. The solid curve gives bounds for exact data, while the dashed curve gives bounds when data errors are less than or equal to 1 mgal. For example, if the source is allowed to reach the surface the density contrast must reach or exceed 0.1 g/cm^3 for exact data, but if it nowhere comes within 4 km of the surface, the density contrast cannot be everywhere less than 0.55 g/cm^3. Also, important for our purposes, the argument can be turned around if an upper bound on the density contrast can be assigned. Thus, if the density contrast is not greater than 0.4 g/cm^3, then the maximum depth of burial is 3.5 km for exact data and 5.25 km for noisy data, because the ideal bodies and therefore all solutions confined to greater depths have densities exceeding 0.4 g/cm^3.

Figure 6 gives density bounds for sources confined between the surface and the specified depth. These curves can be used in a similar fashion, as above, to determine lower bounds on the thickness of the source. For the same maximum density contrast, 0.4 g/cm^3, the minimum thickness is 2.2 km for exact data and 2.0 km for noisy data.

Two oil wells, located on the northwestern flank of the anomaly at SEC 32, T9N, R15W and SEC 17, T9N, R14W, were used to estimate a depth to basement of 1.16 km. An oil well located just to the south of the anomaly at SEC 11, T2N, R16W indicates a depth to basement of 1.67 km. There are no deep wells located over the anomaly. Over the area of the anomaly the sediments are nearly flat or deformed slightly into gentle synclines and anticlines with limbs dipping 3° to 5°. There is no surface evidence to suggest stratigraphic thinning or basement uplift. Consequently, there is no direct evidence for

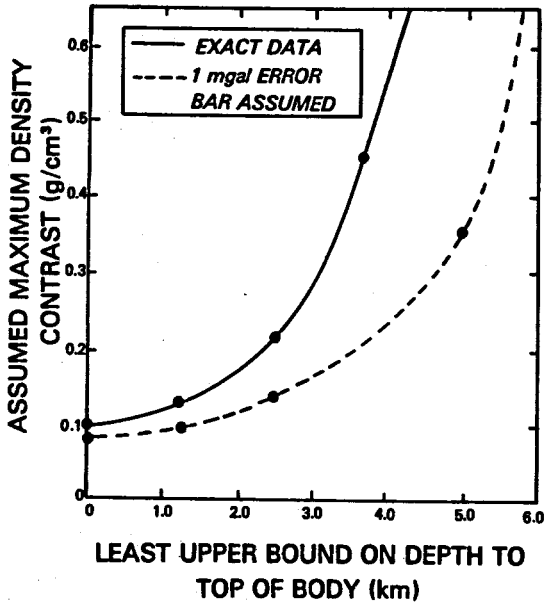

Fig. 5.
Trade-off curve for assumed maximum density contrast vs least upper bound on depth to top of the body for the Chimney Hill gravity profile AA (from Ander[9]).

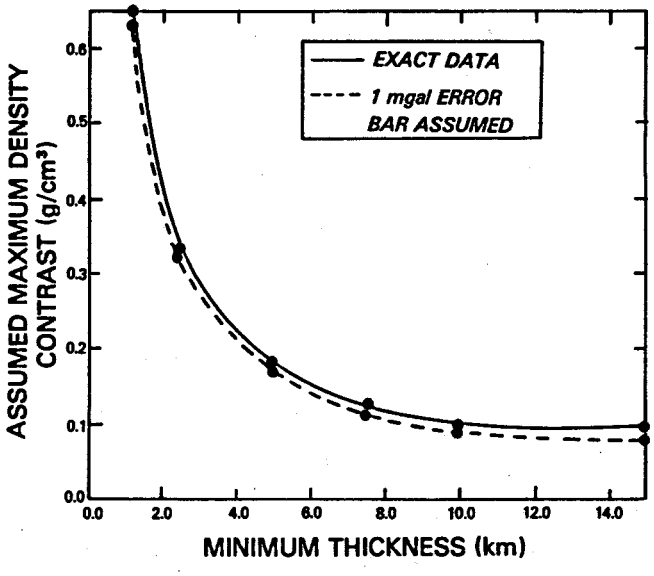

Fig. 6.
Trade-off curve for assumed maximum density contrast vs minimum thickness of body for the Chimney Hill gravity profile AA' (from Ander[9]).

stratigraphic thinning associated with the anomaly. Figure 6, using noisy data, indicates a minimum thickness of 2 km for the anomalous body with a high density contrast of 0.4 g/cm^3, assuming it touches the surface. Thus it is safe to assume that the anomaly is not due to a horst structure. This requires that the anomalous body must be within the basement. If 1.4 km is taken as the average depth to basement and it is further assumed that this is the upper limit on the depth to the top of the body, then 0.14 g/cm^3 is the lowest bound on the maximum density contrast for exact data and 0.105 g/cm^3 for noisy data. Figure 7 gives density bounds for sources confined below 1.4 km depth. Confining the body below 1.4 km does not substantially increase the minimum thickness of the anomalous body. The minimum thickness is 2.25 km for noisy data and 2.5 km for exact data assuming a maximum density contrast of 0.4 g/cm^3.

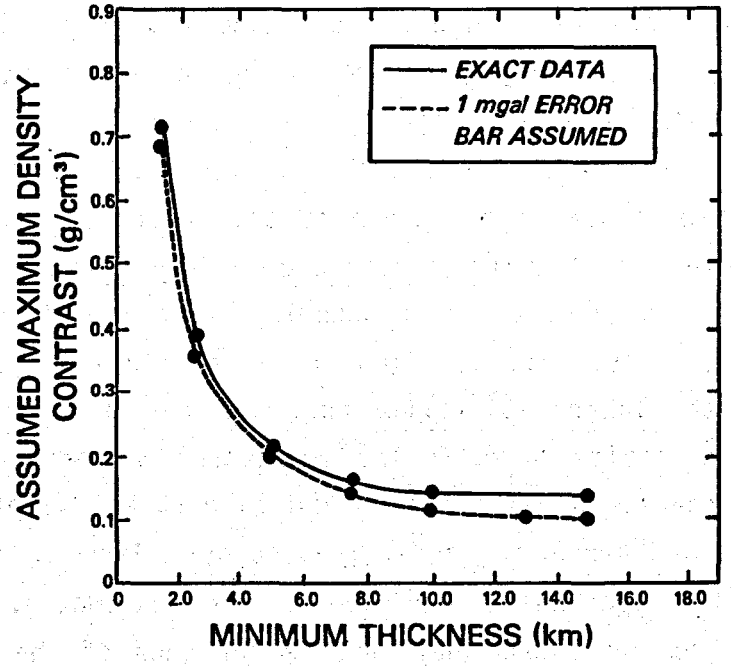

Fig. 7.
Trade-off curve for assumed density contrast vs minimum thickness of body for the Chimney Hill gravity profile AA', assuming the source is confined below 1.4 km depth (from Ander[3]).

VI. REGIONAL MAGNETOTELLURIC STUDY

As part of the hot dry rock geothermal energy resource evaluation effort, the Los Alamos National Laboratory is performing a regional MT survey of west-central New Mexico.[7,8] This survey is focused upon the Jemez volcanic lineament and is part of a much larger regional MT survey of Arizona and New Mexico.[9,12] A detailed discussion of this work is given by Ander.[9] The objective of this study is to map the depth to the electrical conductive layer in the crust and/or upper mantle over a large region. The upper mantle conductive zone is generally believed to be due to partial melting, or possibly to temperature-dependent semiconduction.[36] The crustal conductive zone may be due to partial melting, increased pore fluids, and/or increased temperature.[37,38] The depth to the crustal conductor is arbitrarily assigned as the depth of the 50-ohm-m contour interval.

Preliminary results from the MT survey of west-central New Mexico indicate that the Jemez lineament is associated with a substantial shallowing of the crustal conductor beneath the lineament. The abundance of late Cenozoic volcanism along the lineament suggests that the high electrical conductivity at shallow depths is due to magma intruded along the lineament. In the vicinity of the Zuni-Bandera volcanic field, the crustal conductor is inferred to be no deeper than 10 km, based on one-dimensional analysis of the MT sounding curves. A better estimate of the depth to the crustal conductor will be obtained when two-dimensional analysis of the data is performed.

Figures 8, 9, and 10 give the MT sounding curves obtained at stations 32, 33, and 44, respectively. The locations of these stations are shown in Fig. 3. In each case the lower resistivity curve is the transverse electric mode and the higher resistivity curve is the transverse magnetic mode. Note that useable data are sparse for stations 32 and 33 between 0.1 and 1.0 Hz. This is often the case in MT sounding and is caused by a lack of sufficient signal strength in the MT spectrum to produce reliable estimates. Also shown in these figures is the one-dimensional inverse for each of the sounding curves. The one-dimensional inversions were obtained using the algorithm developed by Anderson.[39] This algorithm uses the Marquart nonlinear least squares inversion technique.

An electrical conductive anomaly, if found to be spacially associated with the body causing the gravity high, might suggest the presence of either partial melt or magma. Within the resolution of the data so far collected,

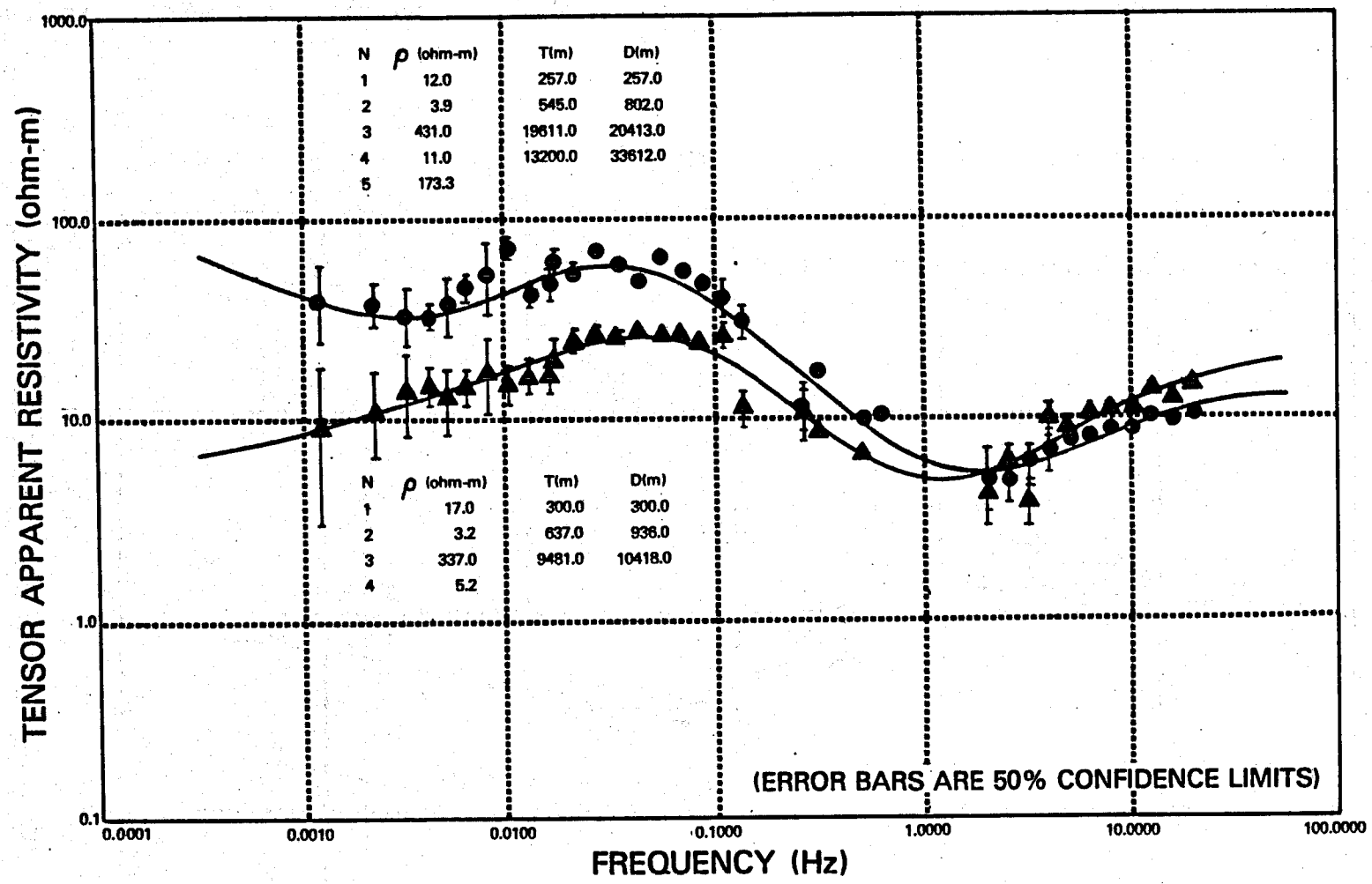

Fig. 8.
Apparent resistivity sounding curves for magnetotelluric station 32 and one-dimensional inversions. T is layer thickness and D is depth to the bottom of the layer.

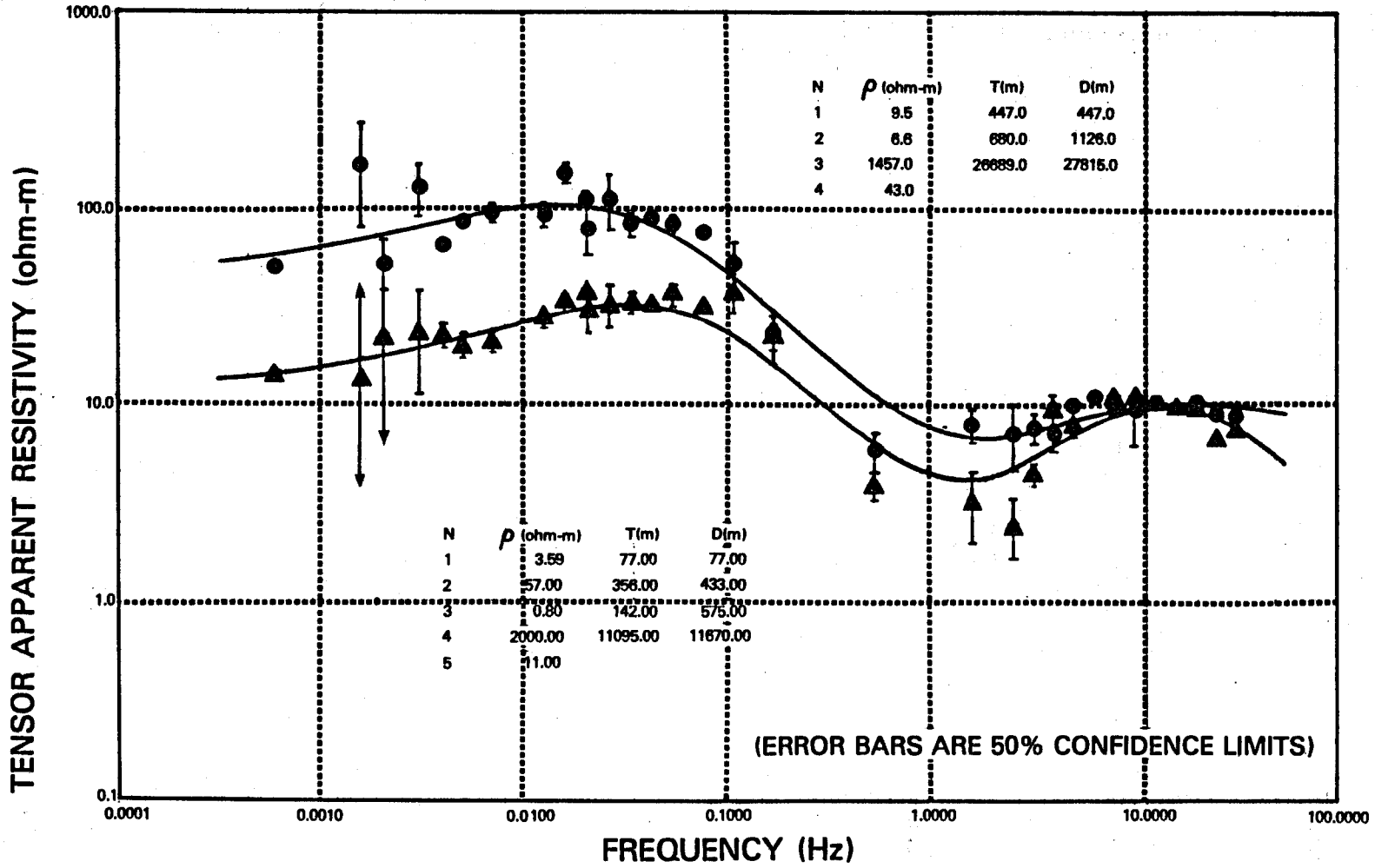

Fig. 9.
Apparent resistivity sounding curves for magnetotelluric station 33 and one-dimensional inversions. T is layer thickness and D is depth to the bottom of the layer.

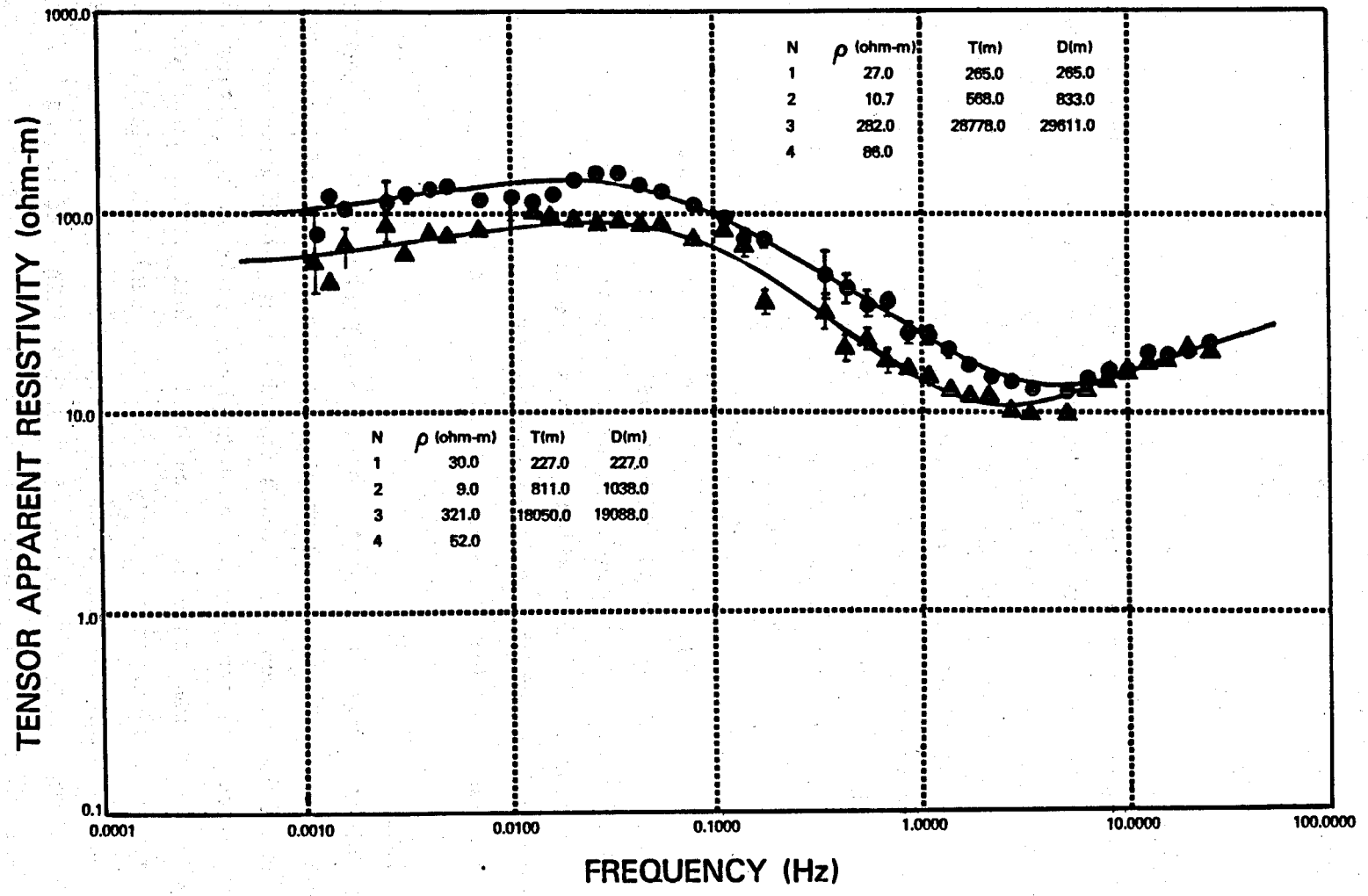

Fig. 10.
Apparent resistivity sounding curves for magnetotelluric station 44 and one-dimensional inversions. T is layer thickness and D is depth to the bottom of the layer.

the MT sounding curves and results of the one-dimensional inversions for stations 32, 33, and 44 do not detect the presence of an upper crustal conductivity anomaly in the basement shallower than 9 km. Thus, MT data do not indicate that the gravity anomaly results from shallow intrusion of recent basaltic magma associated with the Zuni volcanic field.

VII. INTERPRETATION

A shallow mafic intrusion is proposed to account for the large positive gravity anomaly. The age of its emplacement is pre-Pleistocene. Although this large basement structure has not been the source of Quaternary magma, it has controlled the development of the Zuni-Bandera volcanic field, as evidenced by the vent locations and orientations of associated normal faults. The conduits are preferentially developed where the Jemez lineament is obliquely crossed by the eastern boundary (density contrast $\geq$0.1 g/cm^3) of the intrusive body. The structure also exhibits some control on the deformation of the sedimentary rocks. Normal faulting associated with the chain of volcanic vents follows this trend. The Nutria Monocline, a major Laramide structural feature about 45 km long, marks the western boundary of the Zuni uplift. The beds of the monocline have dips as great as 80°, but flatten out abruptly to dips of less than 10° within about 1.5 km of the northwestern boundary of the intrusive structure. The truncation of the strike of the Nutria monocline at the northwest boundary of the positive anomaly may suggest that the intrusive body predates and controls the southern extent of the Nutria monocline.

VIII. CONCLUSIONS

The Zuni volcanic field is one of the major volcanic fields of the Jemez lineament consisting of 74 vents that erupted between 64 and 123 km^3 of basalt between 4 Myr and 1000 yrs ago. The vents for the Zuni field occurred along a trend parallel to the eastern edge of a 90-km-long, 30-km-wide positive gravity anomaly with a maximum residual of 34 mgal. Most vent elongations are also parallel to the edge of this gravity anomaly. Ideal body calculations on the residual anomaly show that the anomalous body must have a maximum density contrast greater than 0.1 g/cm^3, is buried no deeper than 5.25 km and has a minimum thickness of 2 km. The anomalous body is interpreted to be a mafic intrusion. Although the age of emplacement is unknown, MT data suggest that the intrusion is not due to recent basaltic magma associated with the Zuni

volcanic field. There is some suggestion that the intrusion predated and controlled the southern extent of the Nutria monocline, a Laramide feature.

ACKNOWLEDGMENTS

This work was entirely supported by the Hot Dry Rock Geothermal Energy Program conducted by the Los Alamos National Laboratory for the Department of Energy, Division of Geothermal Energy. The authors would like to thank F. E. Goff, W. S. Baldridge, and D. T. Vaniman for their reviews of the manuscript. The MT data were collected, under contract, by Argonaut Enterprises Inc., Denver, Colorado.

APPENDIX A

FIELD SUMMARIES OF BASALT UNITS, ZUNI-BANDERA VOLCANIC FIELD

EL TINTERO. el. 2201 m, NW-1/4 NW-1/4 s.30, T13N, R10W, Bluewater Quad. New Mexico.

This simple vent and circular cinder cone is 100 m high, with a flat, raised apron on the southeast flank. There is no apparent relation of the vent to the local structure, but it may be located along one of the northeast-trending faults visible on the north slope of the Zuni uplift. The cone is characterized by massive bedding, with deposits consisting mostly of highly vesicular glassy bombs up to 20 cm long and very little fine ash or lapilli. Cinders contain 1 to 5% feldspar phenocrysts, 1 to 2 m long, and traces of olivine in glassy or aphanitic groundmass. The cone is covered with a poorly developed soil over caliche-cemented cinders.

CONE ADJACENT TO CERRO COLORADO. el. 2552 m, NE-1/4, s.36, T11N, R12W, Mt. Sedgewick Quad., New Mexico.

A simple cone, about 107 m high is breached to the northeast. There are three erosional remnants of the original cone left. The cone is located on Precambrian metamorphic rocks on the highland along a north-south trending fault. Near the summit are mostly agglutinated bombs, up to 50 cm long. On the cone flanks are mostly small bombs and lapilli, including numerous ribbon

bombs. There are thick, stubby flows to the north, east, and south, along valleys and canyons.

PAXTON SPRINGS CONE. el. 2490 m, SW-1/4, s.25, T1ON, R12W. Paxton Springs Quad., New Mexico.

This cone is about 110 m high, with two small subsidiary cones (both about 20 m high) located south of the main cone. The cones are located along one of the main north-south trending faults that crosses the Zuni highland. Massive cinder beds with blocks up to 20 cm in diameter are exposed in cinder pits located on the southern blank. The cinders are covered with a yellow-brown soil, 0.2 to 1.5 m thick.

OSO RIDGE CONE. el. 2656 m, W-1/2, s.25, T1ON, R12W, Paxton Springs Quad., New Mexico.

This 100-m-high cone is located on a high ridge along a northwest-trending fault. It consists of mostly welded spatter and rootless lava flows and is breached to the north. Bombs in the spatter are up to 2 m long. There are thick, stubby flows emanating from the breached side of the crater.

CERRO BANDERA. el. 2552 m, SW-1/2, s.22, T9N, R12W, Ice Caves Quad., New Mexico.

This cinder cone is breached on the northwest flank, with a spatter and cinder rampart trending north-northeast from it. The sequence visible in the crater walls is of tephra-agglutinate-tephra-cinders. This cone is part of a north-northeast trending chain of craters between Cerro Bandera and Cerro Leonides.

BANDERA CRATER. el. 2533 m, NE-1/4, s.22, T9N, R12W, Paxton Springs and Ice Caves Quad., New Mexico.

This 145-m-high cinder cone is breached on the southwest side. There are some spatter ramparts flanking the breach. There were two periods of eruption. The earlier eruption deposited oxidized cinders with abundant, partly melted xenoliths of Permian sedimentary rocks, and the later episode produced deposits of alkalic basalt containing ultramafic xenoliths (olivine-red spinel and pyroxene-green spinel).[2]

McCARTYS CRATER AND FLOW. el. 2244 m, s.28, T7N, R11W, Ice Caves Se Quad., New Mexico.

This low crater is mostly buried by its own lava flows. According to local history, there was a small cone, but it was destroyed by bombing practice during World War II. The flow covers an area of about 1000 km^2.

LA TETERA. el. 2420 m, W-1/2, s.25, T9N, R12W, Ice Caves Quad., New Mexico.

This basaltic shield, with a collapse crater 120 x 180 m and breached on the northeast flank, consists mostly of cinders. It is located along a buried north-northeast trending fault scarp.

TWIN CRATERS. el. 2423 m, SE-1/4, s.25, T9N, R12W, Ice Caves Quad., New Mexico.

This line of vents actually consists of three craters along a fissure oriented N30°E coincident with a buried normal fault. The highest of the cones is about 73 m and has a small spatter rampart on the north side.

CERRO CANDELARIA. el. 2458 m, center, s.25, T9N, R12W, Ice Caves Quad., New Mexico.

Cerro Candelaria is a cinder and spatter cone 116 m high. It is open to the south where a lava tube begins, trends north, then southeast.[23]

EL CALDERON. el. 2320 m, center-top, s.5, T9N, R11W, and bottom, s. 32, T9N, R11W. Ice Caves Quad., New Mexico.

Two eruptive periods involving cinders have produce this broad, symmetrical cinder cone that is breached on its northeast flank.[40] Numerous lava tubes are associated with this vent.

HOYA DE CIBOLA. el. 2323 m, s.29, T8N, R12W, Ice Caves Quad., New Mexico.

This crater is part of a low shield located east of Cerro Hueco. The vent trends north-northeast and may have formed partly by collapse, producing an elongate crater about 0.6 km long, 0.2 km wide, and 30 m deep.

CERRO ENCIERO. el. 2243 m, S.36, T8N, R12W, Ice Caves Quad., New Mexico.

There is no field description for this older, eroded cone.

CERRO RENDIJA. el. 2494 m, S.5 and 6, T8N, R12W, Ice Caves and Cerro Hueco Quads., New Mexico.

This prominent shield volcano, about 3.75 km wide at the base and 152 m high, is crossed by a chain of small craters and fissures, oriented N14°E. The southernmost of the craters is breached to the south. There are mostly large bombs (around a meter and larger) and welded spatter at the summit along the crater rims. The shield is eroded and has a well-developed soil on its flanks.

CERRITO ARIZONA. el. 2385 m, E-1/2, s.36, T9N, R13W, Cerro Hueco Quad., New Mexico.

This is a broad shield that is part of the western most chain of vents in the field. It is an elongate collapsed crater, 580 by 290 m, trending N34°E. The rim consists of lava flows from less than 1 to 10 m thick, interbedded with some welded spatter.

CERRITO COMADRE. el. 2377 m, SW-1/4, S.1, T8N, R13W, Cerro Hueco Quad., New Mexico.

This low-rimmed volcano consists of two vents, with an orientation of N33°E, in line with Cerrito Arizona. Both vents consist of small, symmetrical cinder cones with craters about 150 m in diameter. The northeast crater is breached to the southwest and the southwest crater is open to the northwest. The deposits consist of steeply dipping spatter and cinders.

CERRO AMERICANO. el. 2460 m, SE-1/4, s.11, T8N, R13W, Cerro Hueco Quad., New Mexico.

The crater of this 143-m-high symmetrical cinder cone is breached to the north. There are some "bumps" around the base that Gawell[31] has interpreted as vents, but they appear to be tumuli or piles of cinders rafted out for a short distance from the cone. There is a well-developed soil and pinon forest on the flanks and summit of the cone. Bombs up to 10 cm long and some blocks (average size 3 cm) are characteristic of the deposits immediately below the soil.

CERRO LEONIDES. el. 2377 m, s.15, T8N, R13W, Cerro Hueco Quad., New Mexico.

The base of this broad, complex cinder cone occupies most of one section. It is characterized by a fault that crosses it with a trend of N18°E. The fault may be a slump scarp associated with partial collapse of the cone; however, there is a low spatter rampart south of the cone that is in line with this fault. The cone is made up of interbedded welded spatter, with bombs up to 1.5 m long, and coarse cinders.

CERRO PIEDRITA. el 2488 m, NW-1/4, S.8, T7N, R13W, Cerro Brillante Quad., New Mexico.

Cerro Piedrita is a semicircular cinder cone, open on the south side. It is slightly asymmetrical along a north-northeast trend. It is surrounded and partly buried by lava flows from Cerro Lobo. The deposits consist of mostly equant bombs and blocks (not welded).

CERRO LOBO. el. 2544 m, SE-1/4, s.8, T7N, R13W, Cerro Hueco Quad., New Mexico.

In this steep-sided cone, the summit is preserved by a well-developed spatter rampart and rootless lava flows at the crater rim. The crater is breached to the west. Stubby flows from this vent make up part of the shield surrounding it, Cerro Chato, and a number of nearby unnamed cones.

HILL 8042. el. 2451 m, center, S.9, T7N, R13W, Cerro Hueco Quad., New Mexico.

This is a rounded, eroded cone remnant with a 400-m-diam crater. The erosional remnant is composed of interbedded spatter and cinders. The low crater rim on the west is composed of spatter ramparts.

CERRO NEGRO. el. 2461 m, W-1/2, S.28, T8N, R13W, Cerro Hueco Quad., New Mexico.

This large cinder cone, 130 m high, is "split" along a north-south line by an arcuate slump scarp. It appears that the cone, highest on the east side, slumped into a collapsed crater on the west side. The slumped material may have been partly buried by later strombolian activity. There are some depressions near the cone that look like elongate craters but are actually kipukas surrounded by steep-sided flows. Far out on the north flank is a ridge that may be an old spatter rampart.

CERRO HUECO. el. 2421 m, SE-1/4, S.26, T8N, R13W, Cerro Hueco Quad., New Mexico.

Cerro Hueco is a broad semicircular cinder cone with a 500- by 600-m crater that is breached on the north side. The crater is about 30 m deeper than the surrounding countryside and exhibits evidence of considerable collapse. Some large blocks of outflow lava at the breach have tilted back into the collapse crater. The cone consists of mainly welded spatter with interbedded cinders. The north crater rim is composed of shelly pahoehoe flows 0.5 to several meters thick.

UNNAMED CONE 2-1/2 Km NW OF CERRO PIEDRITA. el. 2398 m, east 1/2, s.1, T7N, R14W, Cerro Alto Quad., New Mexico.

This crescent-shaped cinder cone is breached on the north-northeast side and is about 400 m in diameter.

CERRO CHATO. el. 2514 m, SE-1/4, s.20, T7N, R13W, Cerro Brillante Quad., New Mexico.

This is a broad, semicircular cinder cone, 166 m high with a crater 550 m in diameter that is breached on the north-northwest side. Crater walls are lined with bedded cinders and welded spatter or agglutinate. Most of the deposits consist of bombs 5 to 10 cm long, with occasional spindle and ribbon bombs.

CERRO CHATITO. el. 2405 m, NE-1/4, s.28, T7N, R13W, Cerro Brillante Quad., New Mexico.

This is a heavily eroded spatter rampart, consisting of bombs and blocks that exist as both welded and unwelded deposits. The cone is surrounded by thick, stubby flows from other cones and is partly buried by them.

CERRO BRILLANTE. el. 2457 m, E-1/2, s.10, W-1/2, s.11, T6N, R13W, Cerro Brillante Quad., New Mexico.

Cerro Brillante consists of two closely spaced vents that define a trend of N42°W. The larger vent, a 171-m-high cinder cone, is breached to the northwest. It consists of mostly welded spatter and interbedded cinders. The small cone on the southeast side of Cerro Brillante, 116 m high, consists of lapilli-size tachylite and sideromelane pyroclasts.

CERRO COLORADO. el. 2401 m, S-1/2, s.32, T7N, R13W, Cerro Brillante Quad., New Mexico.

This older, heavily eroded cone is covered by a soil with rounded, weathered cinders. It is partly buried by flows from cones east and north of it.

CERRO NEGRO. el. 2461 m, NW-1/4, s.31, T7N, R13W, Cerro Brillante and Cerro Alto Quads., New Mexico.

Cerro Negro is a symmetrical cone, 114 m high, with a north-south spatter rampart on the north flank. Its 330-m-diam crater has a small breach on the north side. The deposits are mostly cinders, with a few bombs. It is covered with a well-developed soil and forest on the slopes.

HILL 7981 (Immediately East of Cerro Negro). el. 2433 m, W-1/2, s.29, T7N, R13W, Cerro Brillante Quad., New Mexico.

This is a heavily eroded elongate cone or spatter rampart. If it is a spatter rampart, the elongation may be due to the original shape. The elongation may also be due to erosion along north-south trending faults. The cone is too poorly exposed to determine its original shape.

CERRO FLORA. el. 2424 m, NW-1/4, s.25, T7N, R14W, Cerro Alto Quad., New Mexico.

Cerro Flora is a low cinder cone, breached on the north side. The crater is 300 m in diameter and 76 m high. The cone contains deposits of interbedded spatter and lava flows.

CERRO ORQUETA. el. 2437 m, NW-1/4, s.30, T7N, R13W, Cerro Alto and Cerro Brillante Quads., New Mexico.

This is a cinder cone 81 m high, with a 320-m-diam crater that is breached to the northeast. Although the crater is preserved, the cone is deeply eroded. The slopes are covered with oxidized cinders, blocks, and bombs.

CERRO ALTO. el. 2594 m, s.35, T7N, R14W, Cerro Alto Quad., New Mexico.

Cerro Alto, a 712-m-high symmetrical cinder cone, dominates the countryside as a major landmark. Its shallow crater, 200 m in diameter and about

64 m deep, is breached on the west-southwest side. It is composed of mostly cinders and bombs.

BROAD DEPRESSION SOUTH OF CERRO ALTO. el. 2313 m, parts of s.2,3,10, and 11, T6N, R14W, Cerro Alto Quad., New Mexico.

This 1.2-km-wide, 20- to 30-m-deep crater is an old, eroded maar. Exposures are very poor. On the east rim are a few exposures of beds of lapilli-size basaltic tephra mixed with a few basaltic blocks. The north end of the maar has been filled with flows from Cerro Alto. Along the southwest corner of the maar is a chain of spatter ramparts and cone remnants that form a line of small hills trending N35°E from the south end of the maar. These hills are composed of cinders, bombs, and interbedded basalt flows and are all less than 35 m high.

UNNAMED CINDER CONE (3.7 km south of Cerro Alto). el. 2357 m, s.1/2, s.10, N-1/2 s.15, T6N, R14W, Cerro Alto Quad., New Mexico.

This is a heavily eroded, 55-m-high cinder cone. The rim is preserved by layers of welded spatter.

CERRO MONTOSO. el. 2421 m, s.35,36, T6N, R14W and S.1,2, T5N, R14W, Cerro Pomo Quad., New Mexico.

On the surface of this old, heavily eroded cinder cone, basaltic bombs and cinders are mixed into the soil that covers the cone (there are no good exposures). It appears to have two vent areas; the main one is on the east side with a satellite vent 1.7 km west and 40 m lower. The flanks of the volcano are covered with wind-blown sand.

CERRO CANTINA. el. 2339 m, s.32 and 33, T6N, R14W, Cerro Pomo Quad., New Mexico.

Cerro Cantina is one of many older, deeply eroded cinder cones and spatter ramparts in the area that have been cut by northeast-trending normal faults. It consists of several vents oriented N31°E, parallel to the normal faults.

CERRO POMO. el. 2386 m, s.3 and 4, T5N, R14W, Cerro Pomo Quad., New Mexico.

Cerro Pomo is the youngest-looking cinder cone in the southern part of the Zuni volcanic field. It is a symmetrical cone, 130 m high, with a crater breached to the west. The slopes consist of weathered cinders, blocks, and bombs.

SOKNO LAKE. el. 2256 m, s.19 and 30, T6N, R14W, Cerro Pomo Quad., New Mexico.

Sokno Lake is located in a 700-m-diam, 20- to 25-m deep crater, surrounded by a low rim deposit consisting of basaltic breccia. There are only a few very poor exposures. The maar is open (breached?) on the south-southwest side. Adjacent to the breached end of the crater is a small spatter and cider cone. The line of the maar and spatter cones is parallel to the Peñasco Ridge fault, a normal fault located about 0.5 km east of the maar.

UNNAMED BASALT PLUG NEAR THE GRASSY PLACE. el 2301 m, NW-1/4 s.7, T5N, R14W, Cerro Pomo Quad., New Mexico.

All that remains of this volcano is a deeply eroded basaltic plug along the normal fault that forms the Peñasco Ridge. It is one of many unnamed basaltic vents cut by northeast-trending normal faults in the Zuni volcanic field.

CERRO GATOS. el. 2270 m, s.30, T5N, R13W, La Rendija Quad., New Mexico.

The Cerro Gatos consist of erosional remnants of a low spatter cone oriented north-northeast.

CERROS DE LAS MUJERES. el. 2497 and 2404 m, s. 16,17,18,19,20,21, T5N, R14W, Cerro Pomo Quad., New Mexico.

These two very old, eroded basaltic plugs are oriented N40°W, normal to the general trend of the Zuni volcanic field. These are most likely remnants of a group of vents and dikes that cross from the Datil area to the southern end of the Zuni field. The plugs form steep spires 150 to 240 m above the surrounding countryside. The vertically jointed plugs are surrounded by talus aprons of flocks from the plugs, mixed with cinders and bombs.

APPENDIX B

IDEAL BODY CALCULATIONS

The ideal body code used in performing the calculations consists primarily of a revised simplex algorithm[35] that has been written specifically for this problem and an algorithm for establishing a two-dimensional constraining region, which is divided into rectangular prisms. The following tables give the code input parameters used to build the necessary prisms and to obtain the solution, or objective function. In every case several different prism sizes and constraining regions were used. Only the solutions used in the preparation of the trade-off curves are shown in the tables. Experience obtained from running over 100 such calculations aided in choosing prism sizes and constraining regions that facilitated a very rapid convergence of the objective function.

In Tables B-I and B-II

X = the distance from the origin to the data point in km

B = the magnitude of the residual anomaly at the data point in mgal

M = the designation number for a group of prisms all having the same size

XO = the starting point of each group of prisms in the x-direction in km

D = the depth of the upper bound of each group of prisms in km

DX = the x-dimension of each prism in a particular group in km

DZ = the z-dimension of each prism in a particular group in km

NX = the number of prisms in a group in the x-direction

NZ = the number of prisms in a group in the z-direction

OF = the objective function in g/cm^3.

TABLE B-I

CHIMNEY HILL GRAVITY HIGH
PERFECT DATA CASE

X(km) =	23.75	36.4	42.0	47.5	54.5	63.9	70.5
B(mgals) =	9.15	26.71	32.61	33.53	18.77	7.59	3.15

Trade-off Curve Point	M	XO (km)	D (km)	DX (km)	DZ (km)	NX	NZ	OF(g/cm^3)
1	1	15.0	0.0	2.5	2.5	22	2	0.095
	2	15.0	5.0	2.5	5.0	22	1	
	3	15.0	10.0	5.0	5.0	11	2	
2	1	20.0	1.25	2.5	2.5	18	3	0.135
	2	20.0	8.75	2.5	5.0	18	1	
3	1	20.0	2.5	2.5	2.5	18	3	0.213
	2	20.0	10.0	2.5	5.0	18	1	
4	1	20.0	3.75	1.25	1.25	36	3	0.460
	2	32.5	7.50	2.5	5.0	9	1	
5	1	20.0	0.0	2.5	2.5	20	4	0.105
6	1	15.0	0.0	1.25	2.5	44	3	0.129
7	1	10.0	0.0	1.25	2.5	48	2	0.180
8	1	0.0	0.0	1.25	1.25	76	2	0.334
9	1	0.0	0.0	1.25	0.625	76	2	0.651
10	1	20.0	1.4	1.25	2.5	40	1	0.136
	2	20.0	3.9	2.5	2.5	20	5	
11	1	20.0	1.4	1.25	2.5	40	3	0.136
	2	20.0	8.9	2.5	2.5	20	1	
12	1	20.0	1.4	1.25	2.5	40	3	0.150
13	1	7.5	1.4	1.25	2.5	60	2	0.206
14	1	0.0	1.4	1.25	1.25	76	2	0.374

TABLE B-I (cont)

CHIMNEY HILL GRAVITY HIGH
PERFECT DATA CASE

X(km) =	23.75	36.4	42.0	47.5	54.5	63.9	70.5
B(mgals) =	9.15	26.71	32.61	33.53	18.77	7.59	3.15

Trade-off Curve Point	M	XO (km)	D (km)	DX (km)	DZ (km)	NX	NZ	OF(g/cm^3)
15	1	0.0	1.4	0.625	1.25	152	1	0.715

TABLE B-II

CHIMNEY HILL GRAVITY HIGH
NOISY DATA CASE, 1 MGAL ERROR BAR ASSUMED

X (km) =	23.75	36.4	42.0	47.5	54.5	63.9	70.5
B (mgals) =	9.15	26.71	32.61	33.53	18.77	7.59	3.15

Trade-off Curve Point	M	XO (km)	D (km)	DX (km)	DZ (km)	NX	NZ	OF(g/cm^3)
16	1	20.0	0.0	1.25	2.5	40	1	0.076
	2	20.0	2.5	2.5	2.5	20	3	
	3	20.0	10.0	2.5	5.0	20	1	
	4	20.0	15.0	5.0	5.0	10	2	
17	1	20.0	1.25	1.25	2.5	40	1	0.099
	2	20.0	3.75	2.50	2.5	20	3	
	3	20.0	11.25	2.50	5.0	20	1	
	4	20.0	16.25	5.0	5.0	10	2	
18	1	20.0	2.5	1.25	2.5	40	1	0.137
	2	20.0	5.0	2.5	2.5	20	3	
	3	20.0	12.5	2.5	5.0	20	1	
	4	20.0	17.5	5.0	5.0	10	1	
19	1	20.0	5.0	1.25	1.25	40	4	0.353
20	1	15.0	0.0	1.25	2.5	48	1	0.100
	2	15.0	2.5	2.5	2.5	24	3	
21	1	5.0	0.0	1.25	2.5	56	2	0.124
	2	5.0	5.0	2.50	2.5	28	1	
22	1	5.0	0.0	1.25	1.25	56	2	0.173
	2	5.0	2.5	1.25	2.5	56	1	
23	1	0.0	0.0	1.25	1.25	75	2	0.324
24	1	0.0	0.0	0.625	1.25	140	1	0.632

TABLE B-II (cont)

CHIMNEY HILL GRAVITY HIGH
NOISY DATA CASE, 1 MGAL ERROR BAR ASSUMED

X (km) =	23.75	36.4	42.0	47.5	54.5	63.9	70.5
B (mgals) =	9.15	26.71	32.61	33.53	18.77	7.59	3.15

Trade-off Curve Point	M	XO (km)	D (km)	DX (km)	DZ (km)	NX	NZ	OF(g/cm^3)
25	1	20.0	1.4	1.25	2.5	40	1	0.096
	2	20.0	3.9	2.5	2.5	20	5	
26	1	20.0	1.4	1.25	2.5	40	1	0.093
	2	20.0	3.9	2.5	2.5	20	4	
27	1	7.5	1.4	1.25	2.5	50	2	0.112
	2	7.5	6.4	2.5	2.5	25	2	
28	1	7.5	1.4	1.25	2.5	50	3	0.138
29	1	0.0	1.4	1.25	2.5	76	2	0.192
30	1	0.0	1.4	1.25	1.25	76	2	0.355
31	1	0.0	1.4	0.625	1.25	152	1	0.683

REFERENCES

1. E. B. Mayo, "Lineament Tectonics and Some Ore Districts of the Southwest," Am. Inst. Min. Metall. and Pet. Eng. Trans., 1169-1175 (1958).

2. A. W. Laughlin, D. G. Brookins, and J. D. Causey, "Late Cenozoic Basalts from the Bandera Lava Field, Valencia County, New Mexico," Geol. Soc. Am. Bull. 83, 1543-1552 (1972).

3. R. G. Luedke and R. L. Smith, "Map Showing Distribution, Composition, and Age of Late Cenozoic Volcanic Centers in Arizona and New Mexico," U.S. Geol. Surv. Misc. Inv. Series Map I-1091-A, 1978.

4. E. N. Goddard, "Geologic Map and Sections of the Zuni Mountains Fluorspar District, Valencia County, New Mexico," U.S. Geol. Surv. Misc. Geol. Inv. Map I-454, 1966.

5. C. L. Edwards, M. Reiter, C. Shearer, and W. Young, "Terrestrial Heat Flow and Crustal Radioactivity in Northeastern New Mexico and Southern Colorado," Geol. Soc. Am. Bull. 89, 1341-1350 (1978).

6. D. Levitte and D. T. Gambill, "Geothermal Potential of West-Central New Mexico from Geochemical and Thermal Gradient Data," Los Alamos National Laboratory report LA-8608-MS (1980).

7. M. E. Ander, A. W. Laughlin, R. Furgerson, J. Foster, and D. Strangway, "Magnetotelluric Study of the Zuni HDR Prospect and Jemez Lineament," (Abst.) EOS Trans. Am. Geophys. Union 61, 17 (1980).

8. M. E. Ander, R. Goss, D. Strangway, C. Hillebrand, A. W. Laughlin, and C. Hudson, "Magnetotelluric/Audiomagnetotelluric Study of the Zuni Hot Dry Rock Geothermal Prospect, New Mexico," Trans. Geother. Resour. Counc. 4, 5-8 (1980).

9. M. E. Ander, "Geophysical Study of the Crust and Upper Mantle Beneath the Central Rio Grande Rift and Adjacent Great Plains and Colorado Plateau," Ph.D. Dissertation, University of New Mexico (1980).

10. C. L. V. Aiken and M. E. Ander, "Gravity and Magnetotellurics Applied to Geothermal Exploration and Resource Evaluation in Southwestern United States, Abstract and Timetable, Int. Assoc. of Volcanology and Composition of the Earth's Interior," 17th Gen. Assem. of the Int. Union of Geodesy and Geophysics (1979).

11. M. E. Ander, "MT Exploration in Arizona and New Mexico for HDR Geothermal Using SQUID Magnetometers," Proc. SQUID Applications to Geophysics Workshop (Office of Naval Research, Los Alamos National Laboratory, 1980).

12. C. L. V. Aiken and M. E. Ander, "A Regional Strategy for Geothermal Exploration with Emphasis on Gravity and Magnetotellurics," J. of Volcanol. and Geother. Res. 9, (1981).

13. C. E. Chapin, R. M. Chamberlin, G. R. Osburn, D. W. White, and A. R. Sanford, "Exploration Framework of the Socorro Geothermal Area, New Mexico," in Field Guide to Selected Cauldrons and Mining Districts of the Datil-Mogollon Volcanic Field, New Mexico, C. E. Chapin and W. E. Elstron, Eds., (New Mexico Geol. Soc. Spec. Publ.) No. 7, 115-129 (1978).

14. R. J. Hackman and A. B. Olson, "Geology, Structure, and Uranium Deposits of the Gallup 1° x 2° Quadrangle, New Mexico and Arizona," U.S. Geol. Surv. Misc. Inv. Series Map I-981, 1977.

15. M. N. Machette, "Preliminary Geologic Map of the Socorro 1° x 2° Quadrangle, Central New Mexico," U.S. Geol. Surv. Open File report 78-607 (1978).

16. D. J. Wyant and A. Olson, "Geologic Map of the Albuquerque 1° x 2° Quadrangle, Northwestern New Mexico," U.S. Geol. Surv. Open File report 78-467 (1978).

17. F. Dellachaie, "Chemical and Petrographic Variations in the Cerro Colorado Paxton Springs Basalt Flows, Valencia County, New Mexico," Unpublished M.S. Thesis, Kent State University, 1973.

18. A. W. Laughlin and F. G. West, "The Zuni Mountains, as a Potential Dry Hot Rock Geothermal Energy Site," Los Alamos National Laboratory report LA-6197-MS (1975).

19. M. J. Gawell and A. W. Laughlin, "Chemical and Petrographic Variations in the Cerro Negro-Cerrito Arizona Cinder Cone Lineation, Valencia County, New Mexico," Geol. Soc. Am. Abstracts with Programs 7, 1084 (1975).

20. J. R. Renault, "Major Element Variations in the Potrillo, Carrizozo, and McCartys Basalt Fields, New Mexico," New Mexico Bur. of Mines and Miner. Resour. Circ. 113 (1970).

21. P. W. Lipman and R. H. Moench, "Basalts of the Mt. Taylor Volcanic Field, New Mexico," Geol. Soc. Am. Bull. 83 (1972).

22. R. L. Nichols, "McCarty's Basalt Flow, Valencia County, New Mexico," Geol. Soc. Am. Bull. 57 (1946).

23. A. W. Hathaway and A. K. Herring, "Bandera Lava Tubes of New Mexico and Lunar Implications," Communication of the Lunar and Planetary Laboratory, University of Arizona, Tucson 8, No. 152, 299-327 (1970).

24. M. E. Ander, G. Heiken, J. Eichelberger, and S. Huestis, "Geologic and Geophysical Investigations of the Chimney Hill Gravity High, New Mexico," (Abst.) EOS 60, No. 16, 396 (1979).

25. C. Fries, Jr., "Volumes and Weights of Pyroclastic Material, Lava, and Water Erupted by Paricutin Volcano, Michoacan, Mexico," Trans. Am. Geophys. Union 34, 603-616 (1953).

26. A. W. Laughlin, D. G. Brookins, P. E. Damon, and M. Shafiqullah, "Late Cenozoic Volcanism of the Central Jemez Zone, Arizona-New Mexico," Isochron/West, No. 25 (August 1979).

27. A. W. Laughlin, Los Alamos National Laboratory, personal communication, 1981.

28. P. W. Lipman and H. H. Mehnert, "The Taos Plateau Volcanic Field, Northern Rio Grande Rift, New Mexico," in Rio Grande Rift: Tectonics and Magmatism, R. E. Riecker Ed., Am. Geophys. Union Spec. Publ. (1979).

29. A. W. Laughlin, D. G. Brookins, A. M. Kudo, and J. D. Causey, "Chemical and Strontium Isotope Investigations of Ultramafic Inclusions and Basalt, Bandera Crater, New Mexico," Geochim. Cosmochim. Acta 35 (1971).

30. D. Vaniman, Los Alamos National Laboratory, personal communication, 1979.

31. M. J. Gawell, "Chemical and Petrographic Variations in the Cerro Negro-Cerrito Arizona Cinder Cone Chain, Valencia County, New Mexico," Unpublished M.S. Thesis, Kent State University (1974).

32. R. L. Parker, "Best Bounds on Density and Depth from Gravity Data," Geophysics 39, No. 5 (1974).

33. R. L. Parker, "The Theory of Ideal Bodies for Gravity Interpretation," Geophys. J. R. Astron. Soc. (1975).

34. C. Safon, G. Vasseur, and M. Cuer, "Some Applications of Linear Programming to the Inverse Gravity Problem," Geophysics 42, 1215-1229 (1977).

35. S. I. Gass, Linear Programming, Methods and Applications, 4th Ed. (McGraw Hill, 1975) 406 pp.

36. T. J. Shankland and H. S. Waff, "Partial Melting and Electrical Conductivity Anomalies in the Upper Mantle," J. Geophys. Res. 82, 5409-5417 (1977).

37. W. D. Stanley, J. E. Boehl, F. X. Bostick, and H. W. Smith, "Geothermal Significance of Magnetotelluric Sounding of the Eastern Snake River Plain-Yellowstone Region," J. Geophys. Res. 82, 2501-2514 (1977).

38. I. S. Feldman, "On the Nature of Conductive Layers in the Earth's Crust and Upper Mantle," in Geoelectric and Geothermal Studies, A. Adam, Ed., KAPG Geophysical Monograph (Akademiai Kiado, Budapest, 1976) pp. 721-730.

39. W. L. Anderson, "Program IMSLTW: Marquart Inversion of Plane Wave Frequency Soundings," U.S. Geol. Surv. Open File report 79-586 (1979).

40. J. D. Causey, "Geology, Geochemistry, and Lava Tubes in Quaternary Basalts, Northeastern Part of Zuni Lava Field, Valencia County, New Mexico," M.S. Thesis, University of New Mexico (1970).

☆U.S. GOVERNMENT PRINTING OFFICE: 1981-0-777-022/70

Printed in the United States of America
Available from
National Technical Information Service
US Department of Commerce
5285 Port Royal Road
Springfield, VA 22161

Microfiche $3.50 (A01)

Page Range	Domestic Price	NTIS Price Code	Page Range	Domestic Price	NTIS Price Code	Page Range	Domestic Price	NTIS Price Code	Page Range	Domestic Price	NTIS Price Code
001-025	$ 5.00	A02	151-175	$11.00	A08	301-325	$17.00	A14	451-475	$23.00	A20
026-050	6.00	A03	176-200	12.00	A09	326-350	18.00	A15	476-500	24.00	A21
051-075	7.00	A04	201-225	13.00	A10	351-375	19.00	A16	501-525	25.00	A22
076-100	8.00	A05	226-250	14.00	A11	376-400	20.00	A17	526-550	26.00	A23
101-125	9.00	A06	251-275	15.00	A12	401-425	21.00	A18	551-575	27.00	A24
126-150	10.00	A07	276-300	16.00	A13	426-450	22.00	A19	576-600	28.00	A25
									601-up	†	A99

†Add $1.00 for each additional 25-page increment or portion thereof from 601 pages up.